J. Condensed Matter Nucl. Sci. 4 (2011) 173–187

Research Article

Review of Twenty Years of LENR Research Using Pd/D Co-deposition

Pamela A. Mosier-Boss,* Jack Y. Dea and Frank E. Gordon†
SPAWAR Systems Center Pacific, San Diego, CA 92152, USA

Lawrence P.G. Forsley
JWK International, Annandale, VA 22003, USA

Melvin H. Miles
Dixie State College, St. George, UT 84770, USA

Abstract

In the Pd/D co-deposition process, working and counter electrodes are immersed in a solution of palladium chloride and lithium chloride in deuterated water. Palladium is then electrochemically reduced onto the surface of the working electrode in the presence of evolving deuterium gas. Electrodes prepared by Pd/D co-deposition exhibit highly expanded surfaces consisting of small spherical nodules. Because of this high surface area and electroplating in the presence of deuterium gas, the incubation time to achieve high D/Pd loadings necessary to initiate LENR is orders of magnitude less than required for bulk electrodes. Besides heat, the following nuclear emanations have been detected using Pd/D co-deposition: X-ray emission, tritium production, transmutation, and particle emission. Experimental details and results obtained over a twenty year period of research are discussed.

Keywords: Nuclear products, Pd/D co-deposition
PACS: 14.20.Dh, 78.67.Rb, 68.35.Ct

1. Introduction

On March 23, 1989, Fleischmann and Pons announced, in a press conference, that their electrochemical cells were producing more heat than could be accounted for by chemical means. They speculated that the heat had a nuclear origin. The physics community noted that Fleischmann and Pons had not published their results in any journal prior to their announcement, there had been no reports of any replications of the effect, there was no mention of the generation

*E-mail: pam.boss@navy.mil
†Retired

of any nuclear ash, and that the reported results did not match theory. Despite these deficiencies, scientists, worldwide, went into their laboratories to replicate the Fleischmann–Pons results. A few scientists succeeded but a great many more failed. It is now known that failures were due to the fact that the experimental conditions necessary to achieve the effect, i.e., high D loading and high D flux inside the Pd lattice, had not been achieved.

Stanislaw Szpak, an electrochemist at the Navy laboratory in San Diego, was aware of the Fleischmann–Pons experiment prior to the press conference and knew about the long incubation times needed to fully load bulk Pd with D. To reduce the incubation time, he developed the Pd/D co-deposition process as a means of initiating low energy nuclear reactions (LENR). In this process, working and counter electrodes are immersed in a solution of palladium chloride and lithium chloride in deuterated water. Palladium is then electrochemically reduced onto the surface of the working electrode in the presence of evolving deuterium gas. In this communication, a review is presented of observations made using the Pd/D co-deposition process. The research efforts can be grouped into three time periods for the years encompassing 1989–1995, 1995–2005, and 2005 to present.

2. Summary of Results between 1989 and 1995

In the years between 1989 and 1995, the emphasis of the research was to characterize the deposit formed as the result of Pd/D co-deposition and to search for evidence of nuclear products.

2.1. Characterization of the Pd/D Deposit

The Pd formed as a result of Pd/D co-deposition is black and powdery. Figure 1a shows a scanning electron microscope (SEM) image of an electrode prepared by the Pd/D co-deposition process. It can be seen that the highly expanded surface consists of small spherical nodules [1,2]. Cyclic voltammetry [2,3] and galvanostatic pulsing [4] experiments indicate that, by using the co-deposition technique, a high degree of deuterium loading (with an atomic ratio D/Pd>1) is obtained within seconds and maintained throughout the experiment. These experiments also indicate the existence of a D_2^+ species within the Pd lattice. Because an ever expanding electrode surface is created, non-steady state conditions are assured, the cell geometry is simplified because there is no longer a need for a uniform current distribution on the cathode, and long charging times are eliminated [5].

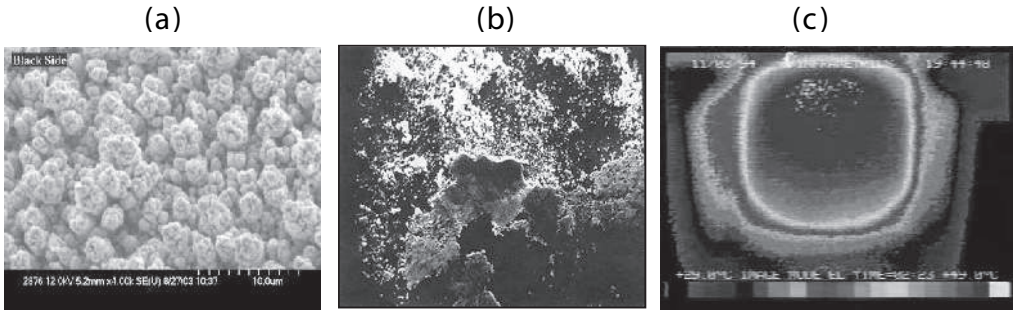

Figure 1. (a) SEM of the Pd deposit formed as the result of Pd/D co-deposition [6] (Reprinted with permission from *Eur. Phys. J. Appl. Phys.*). (b) SEM of the Pd film showing features consistent with Pd melting under water [7] (Reprinted with permission from *Phys. Lett. A*). (c) Infrared image of a cell during Pd/D co-deposition. The circular area in the center is the cathode.

2.2. Evidence of excess heat

In the early experiments, a thermocouple was soldered to the inside of a Cu cathode used as the substrate for Pd/D co-deposition. Another thermocouple was placed inside the cell between the cathode and the anode. Temperature measurements using these thermocouples during electrolysis showed that the cathode was hotter than the solution. These results indicate that the observed heat is not due to Joule heating. In an experiment using Ni screen as the substrate for Pd/D co-deposition, boil off of ~25 mL of solution was observed to occur in a five minute time period. A silver Pd film was observed on the cell wall adjacent to the Ni screen. SEM analysis of this silver film was done (Fig. 1b). According to the metallurgist, Gordon Chase, doing the analysis, the observed features were consistent with metal that had melted under water [8]. The melting point of palladium is 1554.9°C.

In 1994, infrared imaging of the cells was done at UCSD with the assistance of Massoud Simnad of UCSD and Todd Evans of General Atomics. In these experiments Pd/D co-deposition was done on a Ni screen that was in close proximity to a 100 μm thick acetate window [9]. The surface temperature distribution of the backside of the cathode was measured as a function of time using an infrared camera. Figure 1c shows an infrared image of the cell. The circular area is the cathode. It can be seen that the cathode is hotter than the surrounding liquid. It was observed that, unlike Joule heating, excess enthalpy generation occurs in the form of localized events in close proximity to the contact surface. It was also observed that, the higher the electrolyte temperature, the more frequent the events. In the limit, these events overlap to produce oscillating islands. The steepness of the temperature gradients indicates that the heat sources are located in close proximity to the electrode-solution contact surface.

2.3. Measurement of low intensity radiation and tritium content

In 1989, the Department of Energy (DoE) conducted a review of the phenomenon. The conclusions of the review were that the claims of excess heat were not convincing, that the excess heat was not shown to be associated with a nuclear process, and that the evidence of neutron emission was not persuasive. In the aftermath of the DoE review, we concluded that heat was not going to convince anyone that nuclear events were occurring inside the palladium lattice. Also heat does not provide any information as to the processes occurring inside the Pd lattice. For these reasons, the emphasis of our research shifted from heat to looking for nuclear emissions such as γ-/X-rays and tritium.

Pd/D co-deposition experiments were conducted inside lead caves while measuring gamma and X-rays, as a function of time, using a HPGe detector with an Al window and a Si(Li) detector with a Be window [1]. The cathodically polarized Pd/D system was observed to emit X-rays with a broad energy distribution and with an occasional emergence of recognizable peaks attributable to the Pd K_α and Pt L lines. As can be seen in Figure 2a, the emission of γ-/X-rays was sporadic and of limited duration. Photographic film is another detector that has been used to detect radiation. It is an example of a constantly integrating detector, meaning that once an event occurs it gets permanently recorded in the emulsion. Use of a constantly integrating detector is particularly advantageous when events occur sporadically or at low levels, which is true of the Pd/D system. Figure 2b shows photographic film that was placed on top of a thin plastic sheet that was in contact with a silver disk cathode that had been used in a Pd/D co-deposition experiment. The circular shape of the cathode is clearly seen as well as fogging inside the circular disk. The fogging is inhomogeneous indicating that some sites are more active than others.

Figure 3a shows a schematic of the experimental configuration used to monitor tritium in both the liquid and gas phases during electrolysis [10]. In these experiments, the D_2 and O_2 gases were recombined in a separate chamber. The tritium content in the liquid and gas phases were measured daily using the liquid scintillation technique. The measured data were compared to the amount expected based upon mass balance. The time dependence of tritium content of an open cell operating galvanostatically with intermittent sampling is given by the following expression [11]:

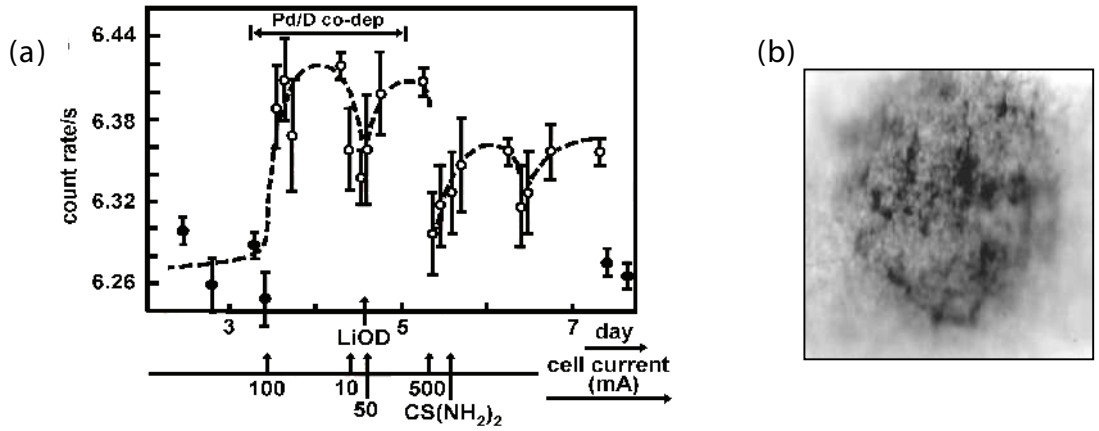

Figure 2. (a) Count rate during cathodic polarization of the Cu/Ag/Pd electrode as measured using a HPGe detector. The period of Pd/D co-deposition is indicated as well as the addition of LiOD and CS(NH2) 2. (b) Fogging of photographic film after exposure to Pd deposited on an Ag disk cathode [6] (Reprinted with permission from *Eur. Phys. J. Appl. Phys.*). A thin Mylar sheet separated the film from the cathode.

$$f(t) = f(0)\left(\frac{m(0) - r(i)t}{m(0)}\right)^{S-1} + \frac{q}{(s-1)r(i)} \bullet \left\{1 - \left[\frac{m(0) - r(i)t}{m(0)}\right]^{S-1}\right\}, \tag{1}$$

where f is the tritium mass fraction, m is the mass of the electrolyte phase, $r(i)$ denotes the rate of change associated with the cell current, q is the rate at which tritium is added/removed, and S is the isotopic separation factor. Figure 3b shows the tritium distribution between the gas and liquid phases observed for one experiment. It was observed that tritium production occurred in bursts and sporadically. During a burst, the rate of tritium production was determined to be 3000–7000 atoms s^{-1}.

3. Summary of Results between 1995 and 2005

In the years between 1995 and 2005, calorimetric measurements were done. Pd/D co-deposition experiments were also done on piezoelectric crystals and triggering of nuclear effects, using external electric and magnetic fields, was examined.

3.1. Calorimetry

Calorimetry of cathodes prepared using Pd/D co-deposition was done by Me l Miles while he was on sabbatical at the New Hydrogen Energy (NHE) Laboratory in Sapporo, Japan [12,13]. He used an isoperibolic Dewar calorimetry cell. The cell was sufficiently tall enough to keep the Pd deposit from reaching the gas-liquid interface thereby preventing D_2 and O_2 recombination from occurring. Results indicated that excess enthalpy was generated during and after the completion of the co-deposition process. The rates of excess enthalpy generated using the co-deposition technique were higher than those obtained using Pd wires or other forms of Pd electrodes. Positive feedback and heat-after-death effects were observed. The rates of excess power generation were found to increase with an increase in both cell current and cell temperature.

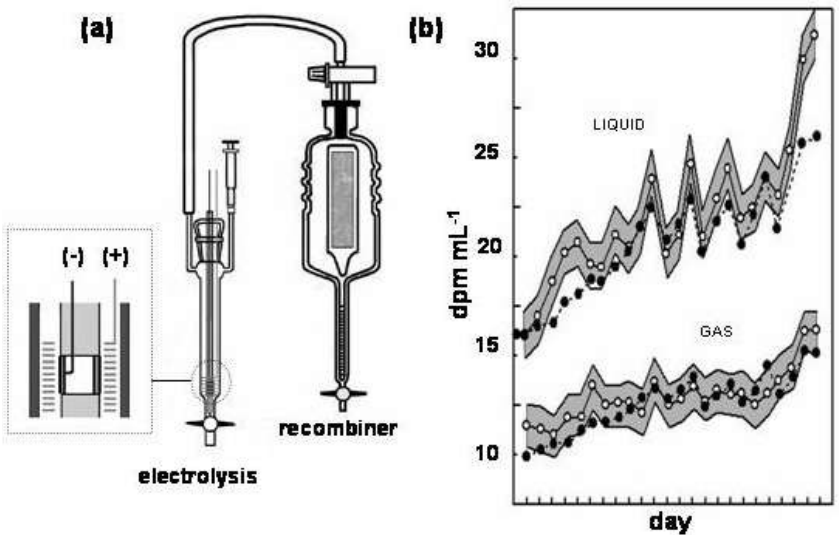

Figure 3. (a) Schematic of the electrolysis cell and recombiner used to monitor tritium in the gas and liquid phases during electrolysis. (b) Tritium content, in dpm mL^{-1}, for Pd/D co-deposition done on a Cu/Ag/Pd cathode. Open circles are the experimental data with the 2σ error bars, solid circles are the amount of tritium expected based upon the mass balance.

3.2. Hot spots and mini-explosions

In 2000, a LENR workshop was held at the then SPAWAR San Diego laboratory. In attendance was Lowell Wood from Lawrence Livermore National Laboratory. Upon seeing the infrared imaging video of the cathode prepared using the Pd/D co-deposition technique, he indicated that the hot spots could be the result of mini-explosions. He further suggested that a microphone in close proximity to the cathode may detect these mini-explosions. Rather than monitoring the experiment with a microphone, a Pb/Zr/Ti piezoelectric crystal was used as the cathode in Pd/D co-deposition. These transducers respond to both pressure and temperature. A schematic of the expected response is shown in Figure 4a. When a mini-explosion occurs, a shock wave, f_1, will be created and heat, Q, will be dissipated. The shock wave is expected to be instantaneous and of short time duration. This shock wave will cause compression of the crystal. The heat will lag behind the shock wave and will cause the crystal to expand. An example of a single event during Pd/D co-deposition is shown in Fig. 4b. A sharp downward spike, indicative of compression caused by the shock wave from the explosion, is observed that is followed by expansion of crystal as the slower heat wave reaches the crystal.

3.3. Triggering: effect of external electric/magnetic fields

In 1993, Bockris et al. [14] reported on three methods of triggering anomalous heat in the Pd/D system. These methods included electrochemical stimulation in which heat bursts were initiated by pulsing the current, radio-frequency stimulation, and magnetic stimulation. Beginning in 2003, the use of external electric and magnetic fields to trigger nuclear processes in Pd/D co-deposition was explored. These efforts are still on-going.

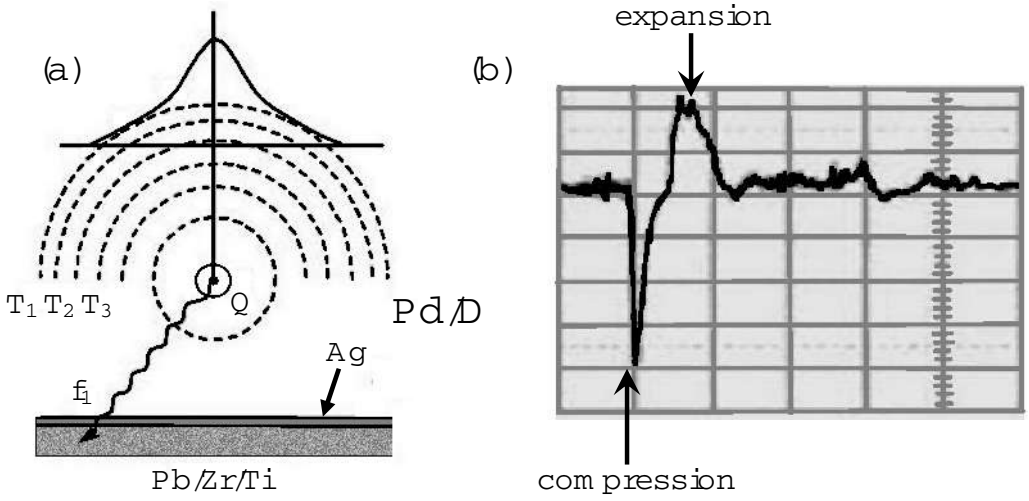

Figure 4. (a) Schematic of the events that should occur when a mini-explosion occurs during Pd/D co-deposition. (b) A recording of a single mini-explosion that was detected using a Pb/Zr/Ti piezoelectric crystal.

3.3.1. *External electric fields*

Figure 5a shows a schematic of the cell configuration used in the external electric field experiments [15]. Copper plates were attached on either side of the cell. A regulated high voltage source was used to apply 6000 V DC (with a ∼ 6 % AC component ripple) across these Cu electrodes. The electric field was applied after Pd/D co-deposition onto an Au foil cathode had been completed. The experiment was terminated after 48 h and the cathode was subjected to SEM analysis. Figure 1a shows an SEM image of the Pd deposit obtained in the absence of an external field. The deposit exhibits a cauliflower like morphology. After exposure to an external electric field, significant changes in the morphology of the Pd/D deposit were observed. Fractal features (Fig. 5b) were observed as well as dendritic growths, rods, wires, and craters (Fig. 5c). Micro-volcano like features, like those in Fig. 5d, were also observed. This kind of damage to metals is consistent with damage seen in materials such as ^{252}Cf which undergoes spontaneous fission. In ^{252}Cf, the volcano like eruptions result from large numbers of spontaneous fissions resulting in 'spike damage.'

The features shown in Fig. 5b–d are suggestive of solidification of molten metal. If the energy needed to melt metal is of a nuclear origin, it should be reflected by the chemical composition of those features. When these features were subjected to further analysis using an energy-dispersive X-ray (EDX) analysis system, the following new elements were detected: Al, Mg, Si. Ca, and Zn [16]. The distribution of these new elements was not uniform and was only associated with these molten formations. This indicates that the new elements were not the result of contamination. In addition, Ca, Al, Mg, and Si cannot be electrochemically plated onto a cathode from an aqueous solution. This provides additional evidence that the new elements were the result of transmutation and not transportation.

3.3.2. *External magnetic fields*

Figure 6a shows a schematic of the cell configuration used in the current external magnetic field experiments [7]. In an external, magnetic field experiment conducted in 1993, an Au wire cathode was wrapped around a capillary tube housing a thermocouple. Another capillary tube, housing a second thermocouple, was placed between the cathode and anode. The orientation of the cathode was perpendicular to the magnetic field and not parallel as shown in Fig. 6a.

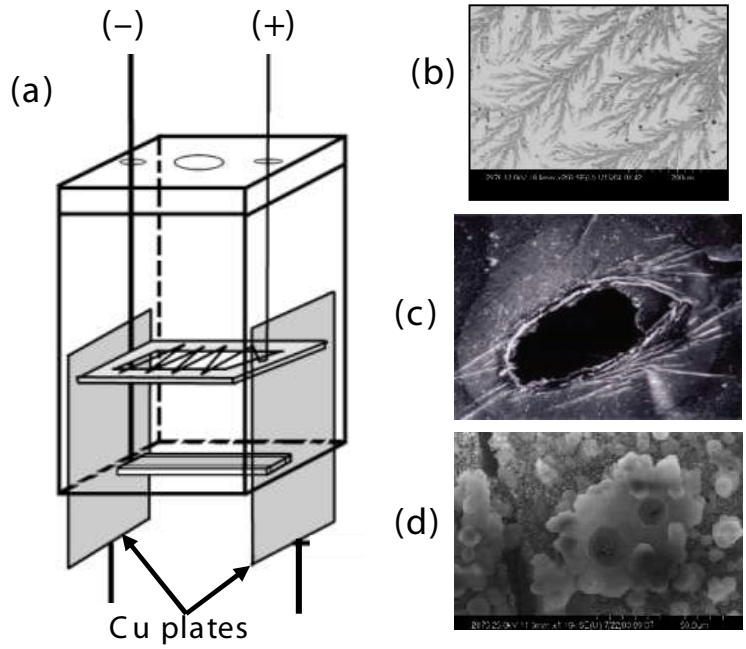

Figure 5. (a) Schematic of the cell used in the external electric field experiment. SEM images of the Pd deposit upon termination of the experiment showing (b) fractals, (c) craters [15] (Reprinted with permission from *J. Electroanal. Chem.*), and (d) micro-volcano like features.

After the Pd had finished plating out on the Au wire, an electromagnet was used to apply a 120 G field. Figure 6b shows the measured temperature response of the thermocouples. Before the electromagnet is turned on, it can be seen that the Au/Pd cathode was hotter than the solution. The temperature differential was approximately 1°C. When the electromagnet was turned on, the temperature of the cathode increased and the temperature differential between the cathode and solution was 3°C. These results were in agreement with what Bockris et al. had observed in his external magnetic field experiments [14].

SEM analysis of the Pd deposit exposed to a 2500 G magnetic field is shown in Fig. 6c. The Lorenz forces of the magnetic field have caused the Pd microglobules to form star-like features. EDX analysis of these features (Fig. 6d) shows the presence of Fe, Ni, Cr, and Al.

Miley and Shrestha [17] have done a compilation of reported transmutation results in LENR experiments. The experiments done include gas permeation of Pd films, electrolytic loading of Pd, and glow discharge. The new elements reported in these experiments are the same as those reported in Pd/D co-deposition. The fact that different experimentalists worldwide, using a variety of deuterium loading procedures, are observing the same elements adds further validation of the results.

4. Summary of Results between 2005 To Present

In 2004 at ICCF14 in Marseille France, George Miley of the University of Illinois Urbana suggested that Pd/D co-deposition experiments should be done using CR-39 as a detector. According to Miley, the CR-39 used in their experiments showed evidence of DD fusion particles. A search of the literature on CR-39 was done. Columbia Resin 39 (CR-39) is an optically clear, amorphous, thermoset plastic. The use of CR-39 to detect nuclear particles was first

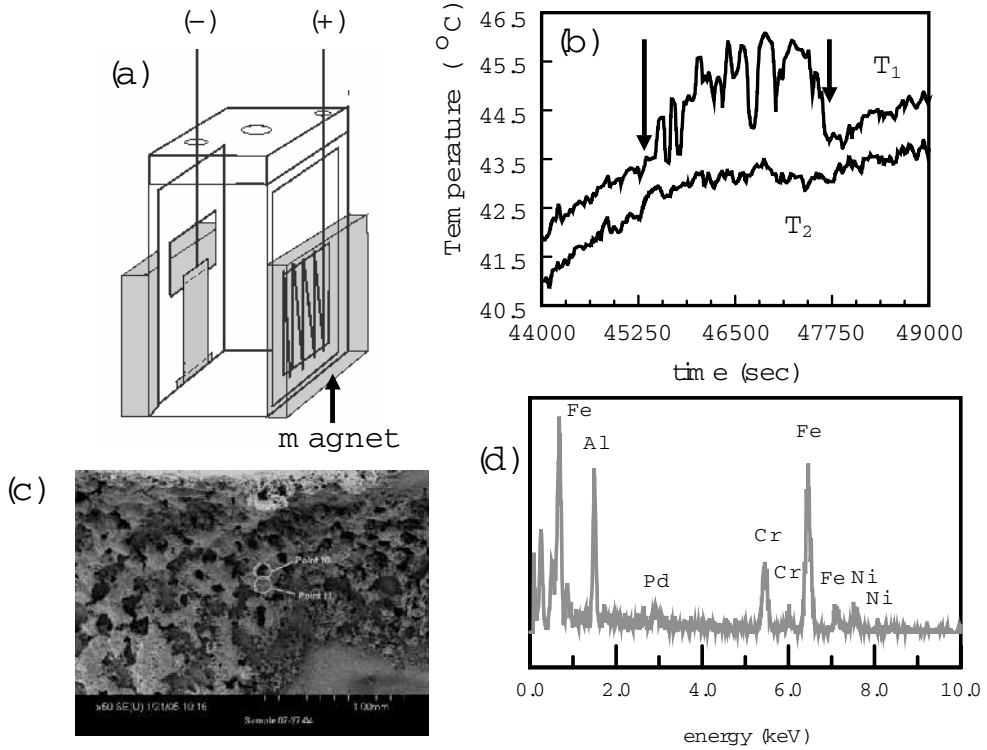

Figure 6. (a) Schematic of the cell used in the current external magnetic field experiment. (b) Temperature response of the Au/Pd cathode (T_1) and solution (T_2) for an experiment conducted in the presence of a 120 G magnetic field. Cell current was at −400 mA. Arrows indicate when the electromagnet was turned on and off. (c) SEM of Pd deposit exposed to a 2500 G external magnetic field. (d) Elemental analysis of point 10 in (c).

demonstrated by Cartwright et al. [18] in 1978. When an energetic, charged particle traverses through a solid state nuclear track detector (SSNTD) such as CR-39, it creates along its path an ionization trail that is more sensitive to chemical etching than the bulk material [18,19]. After treatment with a chemical etchant, tracks due to the energetic particles remain in the form of holes or pits which can be examined with the aid of an optical microscope. The size, depth of penetration, and shape of the track provides information about the mass, charge, energy, and direction of motion of the particle that created the track [20]. Besides detection of charged particles such as protons and alphas, CR-39 can also be used to detect neutrons [21]. In order to detect neutrons with CR-39, the neutron must either scatter or undergo a nuclear reaction with the proton, carbon, or oxygen atoms comprising the SSNTD to form a moving charged particle. It is the track of this neutron-generated charged particle that is revealed upon etching. While most neutrons will pass through without undergoing a reaction, approximately one in 100,000 neutrons passing through 1mm thick CR-39 will create such a track. Other advantages for using CR-39 in Pd/D co-deposition experiments are its integrating capability, which is good for events that occur in bursts or sporadically; the existence of a threshold for registration; ruggedness; insensitivity to electromagnetic noise; and resistance to chemical and mechanical damage.

4.1. Experimental configuration

Figure 7a shows linear energy transfer (LET) curves for charged particles traversing through water. When the cathode emits a charged particle, that charged particle has to traverse through a layer of water before it is registered by the detector. As can be seen, a thin layer of water between the cathode and the detector greatly impacts the charged particle. The larger the charge and size of the particle, the greater the reduction in energy as it travels through the water layer. Also, the deposit formed as a result of Pd/D co-deposition (Fig. 1a) has a cauliflower morphology that will cause the thickness of the water layer to vary. To minimize these effects, the CR-39 detector needs to be in close proximity to the detector as shown in the schematic in Fig. 7b.

4.2. Control experiments

Figure 8a shows damage observed in CR-39 used in a Pd/D co-deposition experiment conducted on an Ag wire in the presence of an external magnetic field. The damage coincides with the placement of the cathode indicating that the cathode is the source of the damage. While the degree of damage looks to be substantial, that is only because CR-39 is a constantly integrating detector. When an event occurs, it gets permanently stamped on the surface of the detector. The damage observed in Fig. 8a had accumulated over a two-week time period. At higher magnification (Fig. 8b) it can be seen that there are circular and elliptical tracks as well as small and large tracks. A triple track is circled. Such tracks result from a reaction that yields three particles of equal mass and energy. The significance of the triple tracks will be discussed vide infra.

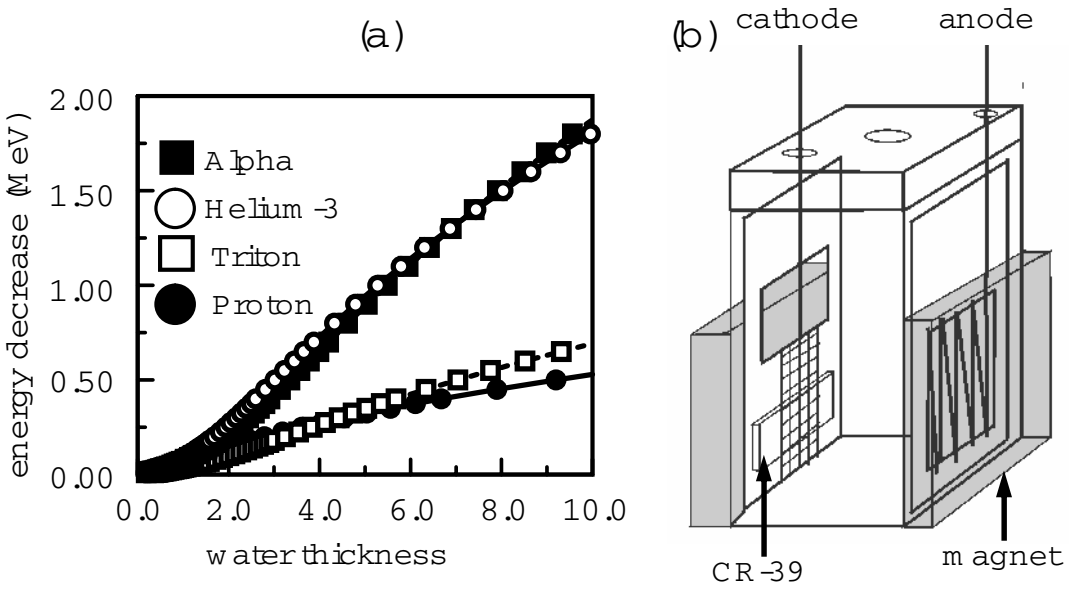

Figure 7. (a) LET curves for charged particles in water. (b) Schematic of the cell.

Figure 8c,d shows tracks obtained in CR-39 resulting from exposure to an ^{241}Am source and Pd/D co-deposition, respectively. The photomicrographs were obtained at 1000× magnification. The top images were obtained by focusing the microscope optics on the surface of the detector and the bottom images are an overlay of two images taken at two

different focusing depths (surface and bottom of the pits). When the microscope optics are focused on the surface of the detector, the pits due to the alpha tracks are dark in color, Fig. 8c top image. Focusing inside the pits, a bright spot is observed, Fig. 8c bottom image. This bright spot is the endpoint of the particle that entered the detector [20]. Tracks have a conical shape. The bright spot inside the track is caused by the tip of the cone acting like a lens when the detector is backlit. These features, dark on the surface and bright spot inside, are diagnostic of a nuclear generated track. As seen in Fig. 8d, the pits obtained as a result of Pd/D co-deposition exhibit these same features. In contrast, features due to chemical damage are bright, shallow, irregular in shape, and exhibit no contrast.

A series of control experiments were conducted to show that the pits resulting from Pd/D co-deposition were not due to either radioactive contamination or to either chemical or mechanical damage [6]. The most notable experiment was replacing the $PdCl_2$ with $CuCl_2$. For both systems, the same electrochemical reactions are occurring. At the cathode, a metal plates out on the electrode substrate and water is reduced to form deuterium gas. Oxygen and chlorine gas evolution occurs at the anode. The only significant difference is that metallic palladium absorbs deuterium and copper does not. Pits were observed for the Pd system and not the Cu. These results indicate that the pits are not due to chemical reactions with the evolving deuterium, oxygen, or chlorine gases; they are not due to the impingement of deuterium gas on the surface of the detector; and they are not due to the metal dendrites piercing into the surface of the detectors.

To determine the energies of the charged particles, experiments were conducted placing 6 μm thick Mylar between the cathode and the CR-39 detector [23]. Approximately 90% reduction in tracks was observed. LET curves indicate that the Mylar film cuts off <0.45 MeV protons and <1.45 MeV alphas. However, this does not take into account

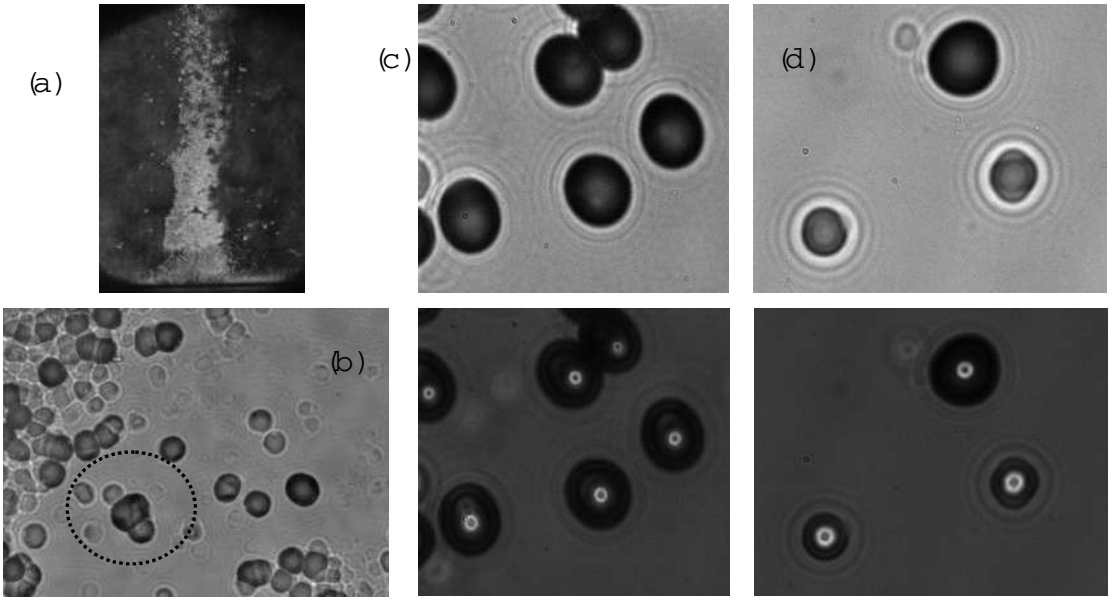

Figure 8. CR-39 photomicrographs of tracks obtained for Pd/D co-deposition done on an Ag wire in the presence of a magnetic field where (a) 20× magnification and (b) 500× magnification. A triple track is circled. (c) and (d) are photomicrographs obtained at 1000× magnification where (c) are tracks resulting from exposure to an ^{241}Am source and (d) are Pd/D co-deposition tracks. In (c) and (d) the top images were obtained by focusing the microscope optics on the surface of the detector and the bottom images are an overlay of two images taken at two different focusing depths (surface and bottom of the pits).

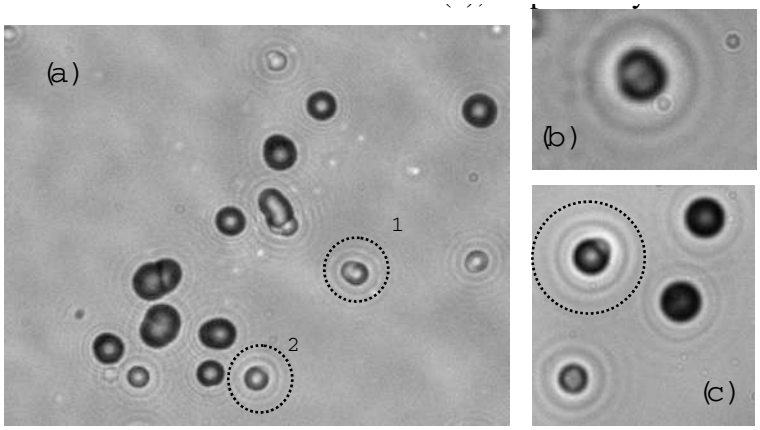

Figure 9. (a) Pd/D co-deposition tracks at 500× magnification. (b) and (c) ∼ 1 MeV alpha tracks obtained by placing 24 μm of Mylar between a CR-39 detector and an ^{241}Am source. Images (b) and (c) taken with a magnification of 1000×. [23] (Reprinted with permission from *Eur. Phys. J. Appl. Phys*.)

the water layer the particle needs to traverse before it reaches the Mylar film. Given the cauliflower-morphology of the Pd deposit, the water film varies between 0 to 10 μm. Taking the water layer into account, the charged particles are primarily <0.45–0.97 MeV protons and <1.45–3.30 MeV alphas. Figure 9 compares Pd/D co-deposition tracks with ∼ 1 MeV alpha tracks. The Pd/D co-deposition tracks, Figure 9a, are primarily circular in shape. There are some elliptically shaped tracks, two of which are circled. Figure 9b,c shows ∼1 MeV alpha tracks. Like the Pd/D co-deposition tracks, these tracks are primarily circular in shape. This indicates that particles traveling at ∼ 90° angle normal to the surface have sufficient energy to get through the water layer and Mylar to impinge on the detector. Particles traveling at oblique angles are blocked. The elliptical ∼1 MeV tracks in 9(b) and circled track in 9(c) look similar to tracks Nos. 1 and 2 in 9(a), respectively.

4.3. Effect of cathode substrate

It was found that the cathode substrate influences the nuclear emissions observed in Pd/D co-deposition. When Pd/D co-deposition was done on a Ni screen in the absence of either an external electric or magnetic field, no tracks were observed in the CR-39 detector [6]. Instead the impression of the Ni screen was observed on the detector. It has been shown that CR-39 can be used in X-ray microscopy [24]. In the contact soft X-ray microscopy technique, the transmission X-ray image of a biological cell was recorded as latent damage on the CR-39 detector. After etching, the image of the cell was revealed as a relief on the polymer. To determine the effect of X and gamma rays on CR-39, experiments were done by exposing Cu-screen covered CR-39 detectors to a ^{137}Cs gamma ray source and to the X-ray source of an X-ray diffractometer. After etching, the impression of the Cu screen was observed in the detectors. These results were similar what was observed in the Ni-screen, no external field, Pd/D co-deposition experiments and suggest that the observed Ni screen damage is due to X-rays/gamma rays. However, when the Pd/D co-deposition experiments on Ni screen were done in the presence of either an external electric or magnetic field, tracks were obtained [6]. In contrast to the Ni screen experiments, tracks were obtained in the CR-39 detectors in Pd/D co-deposition on Ag, Au, and Pt wires in both the presence and absence of an external electric/magnetic field.

To further illustrate the effect of cathode substrate on the observed emissions, Pd/D co-deposition, in the absence of an external electric/magnetic field, was done on the cathode shown in Fig. 10. Half the cathode was a bare Ni screen

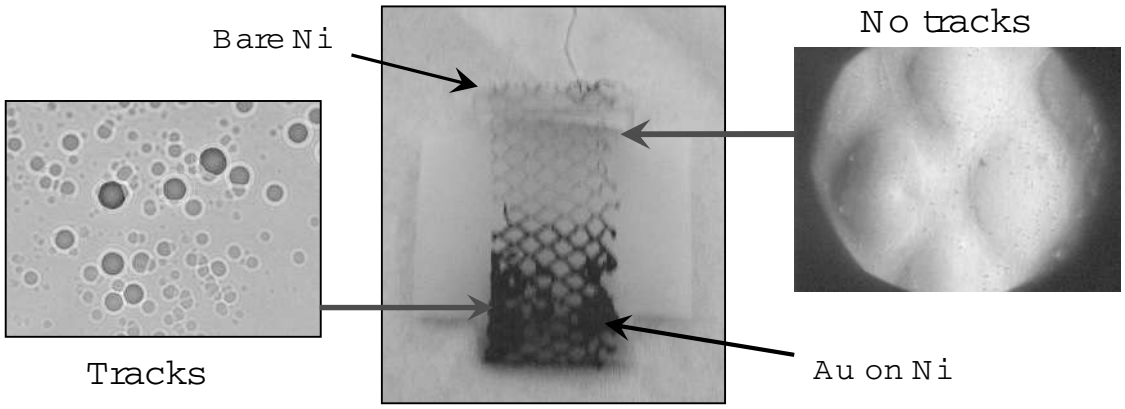

Figure 10. Results obtained on a CR-39 detector used in a Pd/D co-deposition experiment done in the absence of an external field. A photograph of the cathode is shown in the middle. Photomicrographs of the CR-39 are shown.

whereas the other half was Au electroplated onto the Ni screen. Based on prior experimental results, the expectation for this experiment was that the CR-39 detector in contact with the bare Ni would show an impression of the Ni screen whereas tracks would be observed on the Ni/Au half. Figure 10 summarizes the results. Microscopic examination after etching showed that, for the bare Ni half of the cathode, no tracks were observed. Instead, the impression of the Ni screen was observed on the surface of the detector. In contrast, tracks were observed on the Ni/Au half of the cathode. As both halves of the cathode experienced the same experimental conditions, it is difficult to explain such disparate results on chemical damage or radioisotope contamination.

4.4. Evidence of neutrons

In addition to tracks on the front surface of the CR-39 detectors used in Pd/D co-deposition experiments, tracks have also been observed on the backside (Fig. 11a). The detectors are 1 mm thick. The LET curves indicate that the only particles that can go through 1 mm thick CR-39 are >40 MeV alphas, >10 MeV protons, or neutrons. Figure 11b shows tracks in CR-39 created upon exposure to a ^{238}PuO fission source. The tracks are very similar to those shown in Fig. 11a and suggest that the backside tracks are due to neutrons. Specifically, the tracks in Fig. 11a,b are circular in shape. Some tracks are circular with small tails that are due to recoil protons that have exited the CR-39 at an oblique angle. In Fig. 11a,b, there are smaller shallower tracks. These are latent tracks which are due to neutron recoils deeper inside the detector. Additional etching will expose these recoil proton tracks that are deeper inside the plastic as shown in Fig. 11c. The top, 50 μm diameter track was a surface track. After etching away an additional 53 μm of the detector, the two recoil proton tracks deeper inside become visible.

Figure 8b shows a triple track that is circled. In SSNTDs such as CR-39, these triple tracks are indicative of DT neutrons causing a carbon atom to shatter into three alpha particles [25–28]. Figure 11d shows a triple track obtained from a different Pd/D co-deposition experiment. The left hand image of Fig. 11d was obtained by focusing the microscope optics on the surface of the detector. The three lobes of the triple track are clearly visible. The right hand photomicrograph shown in Fig. 11d is an overlay of two images taken with the microscope optics focused on the surface of the detector and the bottom of the pits. From this image, three particles breaking away from a center point are clearly visible. Figure 11e shows a DT neutron generated triple track that is very similar to the Pd/D co-deposition triple track shown in Fig. 11d. The number of triple tracks observed in Pd/D co-deposition is low. At most five to ten total such tracks have been detected on both the front and back surfaces of the detector. Both symmetric and asymmetric triple

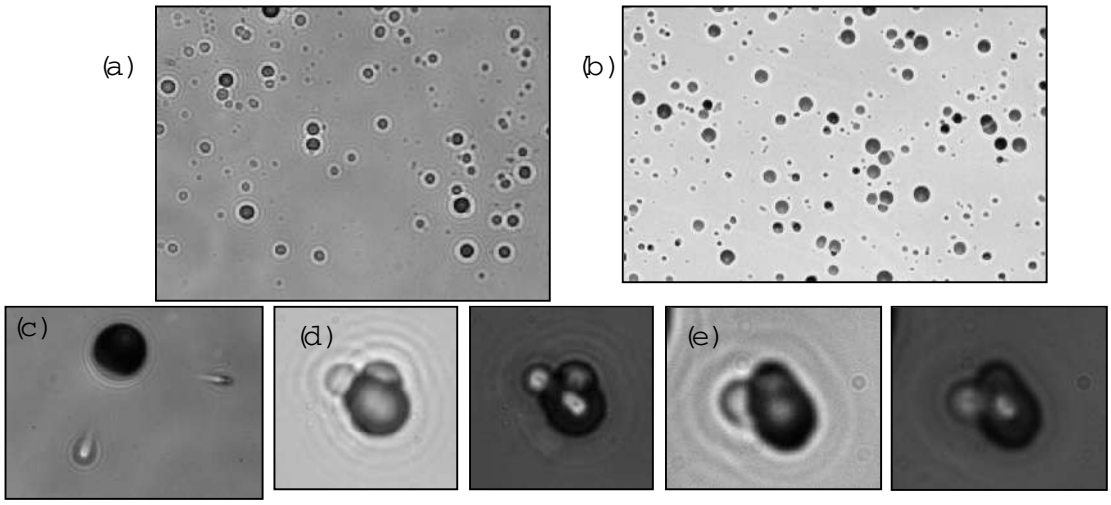

Figure 11. (a) Tracks on the backside of a CR-39 detector used in a Pd/D co-deposition experiment. (b) Tracks in CR-39 caused by neutrons from a ^{238}PuO fission source. (c) Results of sequential etching showing deeper proton recoil tracks. The black, 50 μm diameter track on top is a surface track. Triple tracks obtained as a result of (d) Pd/D co-deposition and (e) exposure to DT neutrons. Left hand images in (d) and (e) obtained with the microscope optics focused on the surface of the detector. Right hand images in (d) and (e) are an overlay of two images taken at two different focusing depths (surface and bottom of the tracks). (c) and (d) reprinted with permission from *Naturwissenshaften* [29].

tracks have been observed in the CR- 39 detectors used in Pd/D co-deposition experiments. The most likely source of the neutrons responsible for the triple tracks is DT fusion inside the Pd lattice.

5. Reproducibility

The SSC-Pacific results using Pd/D co-deposition have been replicated by others. Forsley did infrared imaging of a Ni screen cathode during Pd/D co-deposition and saw that the cathode was hotter than the solution. He also observed that the heat was not homogeneous but occurred as 'hot spots.' Excess heat production in the Pd/D co-deposition system was first measured by Miles [12] and then replicated by Letts [30]. Bockris et al. observed bursts of tritium in the gas and liquid phases using Pd/D co-deposition [31]. Their results were similar to those reported by Szpak et al. [10]. The CR-39 results have been replicated by Kowalski [32], Tanzella et al. [33], and Williams [32]. However, there has been some disagreement as to the origins/interpretations of the tracks observed in the CR-39 detectors used in the Pd/D co-deposition experiments. In particular, Kowalski has stated that the tracks are too large to be due to alpha particles [32,34]. However, both track modeling and the results shown in Figure 9 indicate that the Pd/D co-deposition generated tracks have the same size and shape as $\sim$ 1 MeV alpha tracks. Figure 12 shows a side-by-side comparison of Pd/D co-deposition generated tracks and tracks created in CR-39 exposed to a $\sim$1 MeV alpha source. The tracks are indistinguishable from one another.

Tanzella et al. [33] also conducted experiments placing a 6 ìm Mylar film between the CR-39 detector and the cathode. While a $\sim$90% reduction was observed in the SSC-Pacific experiments [23], Tanzella et al. reported a 99.9% decrease. Kowalski [34] has suggested that this difference is significant. A number of experimental factors, such as the proximity of the wires to the Mylar film, surface area, etc. could explain the reported differences between the SRI and the SSC-Pacific results. In their analysis of Tanzella's CR-39 detectors, Lipson et al. only scanned under-dense track regions to better quantify the energy of the charged particle and recoil tracks. This will result in an undercounting

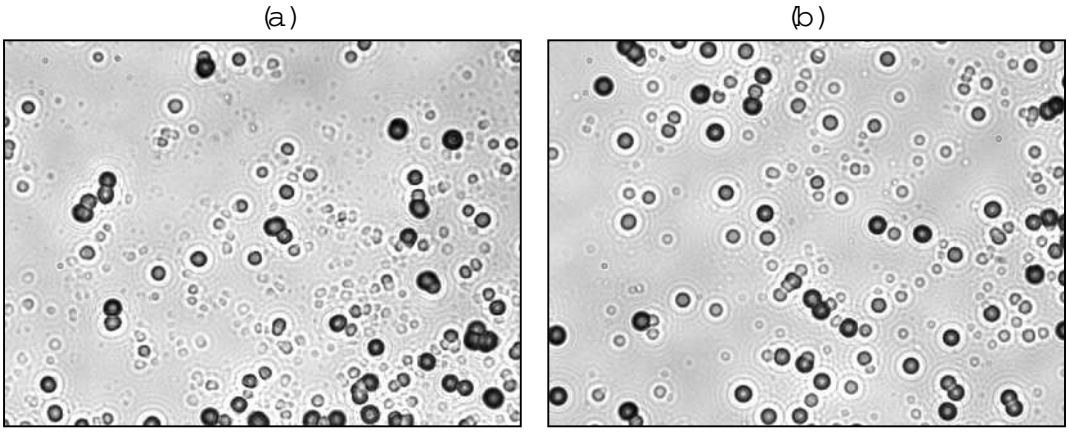

Figure 12. Photomicrographs obtained at 500× magnification for (a) Pd/D codeposition tracks and (b) ∼1 MeV alpha tracks. (a) and (b) reprinted with permission from *J. Condensed Matter Nucl. Sci*. [35].

of tracks. Also different cathode substrates were used in the two experiments. The cathode substrate used in the SRI experiment was Ag while the SSC-Pacific experiment used Pt and Au wires in series. As discussed vide supra, the cathode substrate used in the co-deposition process does affect the emission of the energetic particles. Kowalski [34] has also stated that the particles reported by Tanzella et al. [33] were identified as 2.5 MeV protons. This is not correct. Using a sequential etching protocol, the tracks were attributed to proton recoils resulting from the interaction of the detector with fast neutrons. The energy of the neutrons responsible for these recoils was determined to be 2.5 MeV.

6. Conclusions

Using the Pd/D co-deposition technique developed by Stanislaw Szpak, we have detected excess heat, gamma and X-ray emissions, tritium production, transmutation, charged particles, and neutrons. Taking all the data together, we have compelling evidence that nuclear reactions are stimulated by electro-chemical processes. To date, these observations have been published in 22 peer-reviewed journal papers and two peer-reviewed symposium books.

Acknowledgments

This work was funded by the SPAWAR Systems Center Pacific ILIR and S and T Initiatives Programs, the Defense Threat Reduction Agency (DTRA), and JWK Corporation. The authors acknowledge the contributions of Dr. Stanislaw Szpak, retired from SPAWAR Systems Center Pacific, who pioneered the Pd/D co-deposition process. The authors would like to thank Massoud Simnad and Todd Evans for their assistance in conducting the infrared imaging experiments; Gordon Chase for his analysis of the cathode after the thermal runaway; M. Ashraf Imam of NRL for SEM analysis of cathodes; and Mark Morey, Jim Tinsley, and Paul Hurley of National Security Technologies, LLC for exposing CR-39 to a DT neutron source. They would also like to thank Dr. Gary Phillips, nuclear physicist, retired from the Naval Research Laboratory, for valuable discussions in interpreting the CR-39 data. Finally, they would like to thank Lowell Wood and George Miley for suggesting experiments to detect mini-explosions and energetic particles.

References

[1] S. Szpak, P.A. Mosier-Boss, *Phys. Letts*. A **221** (1996) 141–143.

[2] S. Szpak, P.A. Mosier-Boss, S.R. Scharber, J.J. Smith, *J. Electroanal. Chem*. **337** (1992) 147–163.
[3] S. Szpak, P.A. Mosier-Boss, S.R. Scharber, J.J. Smith, *J. Electroanal. Chem*. **380** (1995) 1–6.
[4] S. Szpak, P.A. Mosier-Boss, J.J. Smith, *J. Electroanal. Chem*. **379** (1994) 121–127.
[5] S. Szpak, P.A. Mosier-Boss, J.J. Smith, *J. Electroanal. Chem.* **302** (1991) 255–260.
[6] P.A. Mosier-Boss, S. Szpak, F.E. Gordon, L.P.G. Forsley, *Eur. Phys. J. Appl. Phys*. **40** (2007) 293–303.
[7] S. Szpak, P.A. Mosier-Boss, J.J. Smith, *Phys. Lett.* A **210** (1996) 382–390.
[8] Gordon Chase, Private communication.
[9] P.A. Mosier-Boss, S. Szpak, *Nuovo Cimento Soc. Ital. Fis*. A **112** (1999) 577–587.
[10] S. Szpak, P.A. Mosier-Boss, R.D. Boss, J.J. Smith, *Fusion Technol.* **33** (1998) 38–51.
[11] S. Szpak, P.A. Mosier-Boss, R.D. Boss, J.J. Smith, *J. Electroanal. Chem.* **373** (1994) 1–9.
[12] S. Szpak, P.A. Mosier-Boss, M. H. Miles, M. Fleischmann, *Thermochimica Acta* **410** (2004) 101–107.
[13] S. Szpak, P.A. Mosier-Boss, M. H. Miles, *Fusion Technol*. **36** (1999) 234–241.
[14] J. O'M. Bockris, R. Sundaresan, Z. Minevski, D. Letts, Triggering of heat and sub-surface changes in Pd–D systems, *The Fourth International Conference on Cold Fusion*, Lahaina, Maui, 1993.
[15] S. Szpak, P.A. Mosier-Boss, C. Young, F.E. Gordon, *J. Electroanal. Chem.* **580** (2005) 284–290.
[16] S. Szpak, P.A. Mosier-Boss, C. Young, F.E. Gordon, *Naturwissenschaften* **92** (2005) 394–397.
[17] G.H. Miley, P. J. Shrestha, Transmutation reactions and associated low-energy nuclear reactions effects in solids, in *Low-Energy Nuclear Reactions Sourcebook*, Vol. I, J. Marwan, S.B. Krivit (eds.), Washington D.C., American Chemical Society, 2008, pp. 173–218.
[18] B.G. Cartwright, E.K. Shirk, P.B. Price, *Nucl. Instr. Meth.* **153** (1978) 457.
[19] J.R. Bhakta, G.D. Hardcastle, J.C.H. Miles, *Radiation Measurements* **30** (1999) 29.
[20] D. Nikezic, K.N. Yu, *Materials Sci. Eng. R* **46** (2004) 51.
[21] J.A. Frenje et al., *Rev. Sci. Instrum.* **73** (2002) 2597.
[22] G.W. Phillips et al., *Radiat. Prot. Dosim.* **120** (2006) 1.
[23] P.A. Mosier-Boss, S. Szpak, F.E. Gordon, L.P.G. Forsley, *Eur. Phys. J. Appl. Phys.* **46** (2009) 30901: 1–12.
[24] K. Amemiya et al., *Nucl. Instrum. Meth. Phys. Rev.* B **187** (2002) 361.
[25] S.A.R. Al-Najjar, A. Abdel-Naby, S.A. Durrani, *Nuclear Tracks* **12** (1986) 611.
[26] A.M. Abdel-Moneim A. Abdel-Naby, *Radiation Measurements* **37** (2003) 15.
[27] J.K. Palfalvi, et al., *Radiation Measurements* **40** (2005) 428.
[28] L. Saj.-Bohus, et al., *Radiation Measurements* **40** (2005) 442.
[29] P.A. Mosier-Boss, S. Szpak, F.E. Gordon, L.P.G. Forsley, *Naturwissenschaften* **96** (2009) 135–142.
[30] D. Letts, Personal communication.
[31] J. O'M. Bockris, C.-C. Chien, D. Hodko, Z. Minevski, Tritium and helium production in palladium electrodes and the fugacity of deuterium therein, *The Third International Conference on Cold Fusion*, Nagoya, Japan, 1992.
[32] L. Kowalski, Eur. Phys. J. Appl. Phys. **44** (2008) 287.
[33] A.G. Lipson, A.S. Roussetski, E.I. Saunin, F. Tanzella, B. Earle, M. McKubre, Analysis of the CR-39 detectors from SRI's SPAWAR/Galileo type electrolysis experiments #7 and #5. Signature of possible neutron emission, *Proceedings of 8th International Workshop on Anomalies in Hydrogen/Deuterium Loaded Metals*, J. Rothwell, P. Mobberley (eds.), 2008, pp. 182–203.
[34] L. Kowalski, *J. Condensed Matter Nucl. Sci*. **3** (2010) 1.
[35] P.A. Mosier-Boss, F.E. Gordon, L.P.G. Forsley, *J. Condensed Matter Nucl. Sci*. **3** (2010) 4.